A kinetic study on hydrochloric acid leaching of nickel from Ni-Al_2O_3 spent catalyst

P.K. Parhi[a], K.H. Park[a*], G. Senanayake [b]

[a] Mineral Resources Research Division, Korea Institute of Geosciences & Mineral Resources (KIGAM), Daejeon 305-350, Republic of Korea
[b] Parker Centre, School of Engineering and Information Technology, Murdoch University, Perth, WA 6150, Australia.

Abstract:

Hydrochloric acid leaching of nickel from spent Ni-Al_2O_3 catalyst (12.7% Ni, 39.2% Al and 0.68% Fe) has been investigated at a range of conditions by varying particle size (50-180 μm), acid concentration (0.025-2 M), pulp density (0.2-0.4% (w/v)) and temperature (293-353 K). Nickel was selectively leached from the catalyst, irrespective of the different conditions. Under the most suitable conditions (1 M HCl, 323 K, stirring at 500 rpm, 50-71 μm particle size), the extent of leaching of Ni and Al after 2 h was 99.9% and 1%, respectively. The XRD pattern of the spent catalyst corresponded to crystalline α-Al_2O_3 along with elemental Ni. The peak due to elemental Ni was absent in the residue sample produced at the optimum leaching conditions, confirming the complete dissolution of Ni from the spent catalyst. The leaching results were well fitted with the shrinking core model with apparent activation energy of 17 kJ/mol in the temperature range of 293-353 K indicating a diffusion controlled reaction.

Key words: Spent Catalyst, Leaching, Nickel, HCl, Kinetics

∗ Corresponding author at: Mineral Resources Research Division, Korea Institute of Geosciences & Mineral Resources (KIGAM), Daejeon 305-350, Republic of Korea
Tel.: +82 42 868 3601, E-mail address: khpark@kigam.re.kr (Kyung-Ho Park)

1. Introduction

Nickel, in the form of metal, oxide or sulfide, has wide applications in catalysts used in the petroleum industry and several other commercial processes such as: (i) hydrogenation,

hydrodesulphurization, hydrorefining including fat hardening process (Ni-Mo/Al_2O_3, NiO/Al_2O_3, Raney nickel alloy), (ii) refinery hydro-cracking (NiS, WS_3/$SiO_2Al_2O_3$), and (iii) methanation of carbon dioxide from hydrogen and ammonia synthesis gases (NiO/Al_2O_3, $NiSiO_2$) [1]. Nickel metal is found to be the active ingredient in most commercial catalysts and its content varies from 10-25% (w/w) according to operating conditions and type of process [2]. The spent petroleum catalysts for desulfurization of the various fractions, during the refining of petroleum products from the crude [3,4] are considered as a major secondary source of nickel. After several cycles, these catalysts gradually loose the activity as a result of the accumulation of S, C, V, Fe, Mo, Si, As and P on the catalytic surface [5]. Due to the presence of soluble organic and inorganic compounds, the spent catalysts are harmful to the environment. They are classified as hazardous materials restricting the use in land fills and direct disposal [6, 7].

Recycling of these secondary resources, namely spent catalysts, in order to lower their production costs, reduce waste and prevent the environmental pollution has become a necessity. Moreover, the spent catalysts are regarded as one of the best potential sources of metals such as Ni, Mo, V, Co and Al [8]. The increasing demand of the nickel metal has also necessitated its extraction from the secondary resources. The final wastes obtained after recovery of the metal values from the spent waste catalyst are found to be less toxic than the original form [6, 12]. Therefore, much attention is being given towards the development of comprehensive utilization schemes by various processes for metal extraction from spent hydro-processing catalysts to avoid pollution in land disposal and to minimize the landfill space [3, 9-11].

Hydrometallurgical flow sheets for the recovery of metal values from the spent catalysts are considered as environmental-friendly and attribute to low energy consumption, low gas emissions, low waste generations and complete recovery of metals [12]. The processing of spent catalyst can be conducted by indirect or direct methods. In indirect methods, the spent catalysts are

subjected to a pretreatment (oxidation, roasting or baking) process in the presence of solid, liquid or gaseous oxidant to liberate the valuable metal oxides from sulfide based spent catalysts, followed by water/acid treatment depending on the requirements [4,13]. These pretreatment operations, considered as intermediate stages, are time consuming and may lead to unfavourable economics. In contrast, the direct method involves the use of mineral acids or alkali as lixiviants for the leaching of metals from spent catalysts. Overall leaching efficiency from direct method was found to be satisfactory in the case of spent catalysts which consist of metals or metal oxides [12].

A number of acidic reagents, such as HCl, $H_2C_2O_4$, H_2SO_4, HNO_3 and H_2O_2 have been used as the lixiviant to leach metal values in spent catalysts [8, 10, 13-15]. Despite the high efficiency, the leaching with these reagents can consume high energy if operated at high temperatures over long reaction times [12]. Moreover, the leaching of the spent catalysts with mineral acids such as H_2SO_4 and HNO_3 is less selective as they extract large quantities of Al along with Mo, Ni or Co. This causes complications on the downstream separation and purification operations and lengthens the flowsheet.

The recovery of valuable metals from spent catalysts using HCl, developed by Chaudhary et al. (1993) [12], seems to be an attractive and promising option. The use of HCl is advantageous due to its selectivity and favourable economics. It has also been recognized as an effective lixivant for the dissolution of base metal values from various sulfidic, oxidic and metallic resources [16]. However, kinetic studies on leaching of metals from spent catalysts using HCl is limited [15, 17] compared to the studies using other acidic/alkaline reagents. This paper investigates the kinetics of nickel leaching from spent catalyst (Ni/α-Al_2O_3) with HCl by varying the process parameters such as leaching time, stirring speed, acid concentration, temperature and particle size at a low pulp density.

2. Experimental

2.1 Materials and apparatus

The Ni/α-Al_2O_3 catalyst was procured from a Korean refinery plant. The metal contents of the spent catalyst were determined by ICP-AES (JOBIN-YVON JY 38) after complete digestion with concentrated HF. The samples obtained in the leaching tests were also analyzed to determine the metal ion concentration by ICP-AES. The sulfur and carbon contents of the original spent catalyst were determined by using LECOSD-432 Analyzer following the standard procedure. The XRD spectra of spent catalyst as well as some of the leach residues were recorded by using a Rigaku RU-200 spectrometer (Rigaku RTC-300, Co. Japan). Leaching tests were carried out using a three necked 500 ml round bottom flask. Heating and stirring were provided by a temperature controlled mantle heater (accuracy ±1 ^{o}C) and an externally placed variable speed stirrer motor, respectively.

2.2 Leaching procedure and conditions

The lixiviant was heated with stirring at 500 rpm. After attainment of desired leaching temperature the spent catalyst sample of the appropriate particle size range was charged into the flask containing 500 ml of the HCl solution. The effect of changing one of the five parameters: (i) pulp density, (ii) rotation speed, (iii) acid strength, (iv) temperature and (v) particle size range was investigated. Table 1 summarizes the different conditions used in the present study, where one of the parameters was changed in the described range while other parameters were maintained constant. The effect of stirring speed was tested at 200-600 rpm. The average particle size of the spent catalyst was −100 mesh (-147 μm) in most of the experiments, except when the effect of particle size was studied in the range of -50 to -250 mesh (50 to 180 μm). The acid concentration was 1 M HCl, except when the effect of acid strength was studied at the concentration range of 0.025-2.0 M. The pulp density was maintained low at 0.2% or 0.4% solids (w/v).

2.3 Treatment of samples

Slurry samples of 5 ml were withdrawn at regular time intervals, filtered, diluted and analyzed for metal content by ICP-AES. At the end of leaching tests, the slurry was filtered under vacuum, followed by in-situ washing of the residues with de-ionized water. The washed residues were dried in an oven at 100^{o}C overnight, weighed and analyzed for their metal content after digestion. Extent of leaching was calculated on the basis of both solution and solid assays. Some of the leaching tests were repeated in order to ascertain the reproducibility of the experimental results.

3. Results and Discussions

3.1. Characterization of spent catalyst and leach residues

The supplied spent catalyst sample was free from oil and grease materials and the total water soluble fraction was found to be less than 1%. The chemical assay of the sample is shown in Table 2. The original spent catalyst comprises of elemental nickel and α-Al_2O_3 as revealed by the XRD pattern in Fig.1. The XRD pattern of the leach residue obtained using the experimental conditions: temperature 323 K, particle size 50-71 μm, pulp density 0.2% (w/v), HCl concentration 1 M and stirring speed 500 rpm after 120 min, is shown in Fig. 2. The absence of a characteristic peak of crystalline elemental nickel in the leach residue indicates the complete dissolution of nickel metal from the original spent catalyst. Thermodynamic data from the HSC 6.1 database [18] predicts large equilibrium constants for the acid dissolution of both Ni and Al_2O_3 according to the reactions listed in Table 3 at the temperature range 293-353 K. However, the fact that Al_2O_3 remains largely unreacted in the leach residue in Fig. 2 indicates slow reaction kinetics of Al_2O_3. The low dissolution of alumina can also be attributed to the nature of alumina (α-alumina) of original spent catalyst (Fig.1). The solubility of α-alumina is much lower compared to γ-alumina [12].

3.2 Effect of leaching variables

3.2.1 Leaching time and pulp density

As shown in Fig.3, the extraction of Ni in a solution of 1 M HCl stirred at 500 rpm at a temperature of 323 K reached ~84% after 120 min and remained unaffected afterwards. In contrast, the extraction of Al remained unchanged (~1%) over time. All the other experiments were carried out over a time period of 180 min. The acid concentration plays a key role in the dissolution process of the metal from spent catalyst [26]. Therefore, the solid/liquid ratio of the present investigation was deliberately kept low (0.2-0.4% w/v or 2-4 g/L), as in previous studies [27], in order to assure that the reagent concentration remain relatively unchanged due to low consumption. Moreover, the increase in pulp density from 0.2% to 0.4% caused no significant effect on Ni leaching at a given acid concentration of 1 M HCl (Fig. 3). Consequently, the kinetics of nickel dissolution as a function of initial acid concentration could easily be established in the present study, by conducting subsequent experiments at a pulp density of 0.2% and variable acid concentrations as described later.

3.2.2 Stirring speed

As shown in Fig.4, the extraction of Ni in 1 M HCl at 323 K after 180 min was increased from 73% to 82% with an increase in the stirring speed from 200 to 500 rpm. A further increase in the stirring speed to 600 rpm caused no significant increase in Ni extraction. The stirring speed of 500 rpm was maintained for subsequent experiments in order to assure invariance of this parameter.

3.2.3 Hydrochloric acid concentration

Based on the Ni grade of 12.75% in spent catalyst, the stoichiometric acid concentration required for complete dissolution of Ni at a pulp density 0.2% (w/v) is ≈ 0.01 M HCl. Therefore, the acid concentration was maintained excess in the range 0.025 – 2 M at this pulp density to

assure that it was not a limiting factor for the extent of Ni dissolution. The extraction of Ni after 180 min increased from ~40% to ~88% with an increase in the HCl concentration from 0.025 to 2.0 M, as shown in Fig. 5. According to this data the Ni extraction (%) doubled when acid concentration was increased 80 times. These results show the beneficial effect of high acid concentration on kinetics of Ni extraction, as reported by previous researchers [12, 19, 26]. However, despite the increase in initial Ni extraction with the increase in acid concentration the leaching curves reached plateau after 100 min at acid concentrations greater than 0.5 M. This indicates surface blockage which can be rationalized using a shrinking core kinetic model [27] as described later. The extraction of Al was observed to be a negligibly small quantity (~1%), even at high acid concentrations, and it is not included in the figure. All further experiments were carried out using 1 M HCl.

3.2.4 Temperature

The leaching curves of nickel at different temperatures are shown in Fig.6. The increase in temperature has a strong beneficial effect on nickel leaching with an increase in extraction from 69% at 293 K to 97% at 353 K. In turn, the extraction of aluminum also increased by approximately 1-2% with the increase in temperature.

3.2.5 Particle size

A decrease in particle size caused an increase in nickel extraction as shown in Fig.7. The smaller particle size range of 50-71 μm tested in the present study resulted a leaching efficiency of 99.9% after 60 min. This can generally be related to the increase in surface area with finer particles. These results are also consistent with the observations reported for leaching of metal values from the spent nickel oxide catalyst [19].

3.3 Leaching kinetics

Kinetic modeling yields comprehensive information regarding the leaching mechanism for a heterogeneous reaction: A(aq) + bB(s) → products. In acidic leaching, the heterogeneous reaction kinetics for most of the metals in spent catalysts can be interpreted by using shrinking sphere/core models [19]. Based on the results of Ni leaching (%) as a function of time, acid concentration, particle size and temperature at different time intervals summarized in Figs. 3, 5, 6 and 7, the fraction of metal reacted (X) was calculated using Eq. 1. The values of X were fitted to shrinking sphere/core models in Eqs. 2-3 to determine the apparent rate constants and to rationalize the effect of temperature using Eq. 4:

X = % Nickel extraction / 100 (1)

$$1 - (1 - X)^{1/3} = \left[\frac{2bk_i c}{\rho d_o}\right] t = k_{ap} t \quad (2)$$

$$1 - \frac{2}{3}X - (1 - X)^{2/3} = \left[\frac{8bDc}{(1 - \varepsilon)\rho d_o^2}\right] t = k_{ap} t \quad (3)$$

$$\ln k_{ap} = \ln A - \left[\frac{E_a}{RT}\right] \quad (4)$$

where k_{ap} = apparent rate constant, k_i = intrinsic rate constant of the surface reaction (cm s^{-1}), b = stoichiometric factor, c = concentration of reactant (mol cm^{-3}), ρ = molar density (mol cm^{-3}) of the dissolving metal in the particle, d_o (cm) = particle diameter, D = diffusivity (cm^2 s^{-1}) of the species through a product layer, ε = particle porosity, A = pre-exponential factor, R = gas constant (8.314 J/(mol K) and E_a = activation energy (kJ/mol) [20,21].

A shrinking sphere model (Eq.2) assumes that a surface chemical reaction is the rate controlling step while a shrinking core model (Eq.3) assumes that the diffusion of a reactive species or product through a porous solid layer of increasing thickness is the rate controlling step. The leaching results in Fig. 3 were used in Eq. 1 to calculate X, $1-(1-X)^{1/3}$ and $1-2/3X-(1-X)^{2/3}$ and

plotted in Fig. 8 to examine the validity of Eqs. 2 and 3. The linear relationship in Fig. 8 indicates that the leaching reaction is controlled by the diffusion of reactants or products according to the shrinking core model (Eq. 3). The key parameters like temperature, particle size and acid concentration were found to have a significant effect on the apparent rate constant in Eq. 3, as revealed by the change in slopes shown in Figs. 9, 10 and 11, with the change in leaching conditions.

Previously reported low values (<24 kJ/mol) for the activation energy of diffusion controlled reactions are: 4-12 kJ/mol [22, 23], 8-20 kJ/mol [24] and 12-24 kJ/mol [25]. In contrast a leaching process controlled by a surface chemical reaction has higher activation energies: 40-80 kJ/mol [24]. The Arrhenius plot in Fig.12 (Eq. 4) is based on the apparent rate constants determined from the slopes of linear relationships in Fig.9. The slope of the straight line in Fig. 12 corresponds to an apparent activation energy of $E_a = 17 \pm 3$ kJ/mol in the temperature range of 298-353 K, indicating that the rate of leaching is controlled by a diffusion process. The low value of E_a in the present investigation is also consistent with $E_a = 13$ kJ/mol reported for the leaching of pure nickel powder in aqueous chlorine solutions [16].

The apparent rate constant for leaching based on the slopes of the linear relationships in Fig.10 increases with the decrease in particle size of the spent catalyst. A plot of k_{ap} as a function $1/d_o^2$ according to Eq. 3 yields a linear relationship in Fig. 13 with a correlation coefficient of $R^2 = 0.99$ and supports the proposed diffusion controlled mechanism for leaching. The effect of acid concentration on the apparent rate constant is examined in Fig. 14 by plotting log k_{ap} from Fig. 11 as a function of log [HCl]. The slope of ~0.8, close to unity, at low concentrations is consistent with Eq. 3, indicating that the diffusion of H^+ ions through a porous solid is rate controlling. The shrinking core model assumes that while the initial particle size remains relatively unchanged during the reaction a porous product layer builds up around the particle being leached. Previous

studies with nickel laterite ores have shown that the value of k_{ap} increases with acid concentration and the increase in porosity of the ore matrix [28, 29]. However, despite the applicability of a shrinking core kinetic model for the spent catalyst in the present study for all concentrations shown in Fig. 11 and, confirmed by the effect of initial particle size in Figure 13, the values of k_{ap} becomes relatively independent of acid concentrations greater than 0.1 M (Fig. 14). This behavior can be related to a number of reasons: (i) the use of a spent catalyst sample of -80 mesh (-147 μm) to investigate the effect of acid concentration, instead of the particles of narrow size range used to investigate the effect of particle size (Table 2), (ii) the variation of porosity and density of the sample during the reaction at higher acid concentration which in turn can have detrimental effects on the diffusion of H^+ ions, as reflected by a lower value of k_{ap} than expected, at higher acid concentration. Further work is warranted.

4. Summary and conclusion

The XRD analysis of the spent catalyst (feed material) shows peaks corresponding to both Ni and α-Al_2O_3. Thermodynamic calculations based on the HSC 6.1 database predict large equilibrium constants for the dissolution of both Ni and Al_2O_3 by HCl to produce Ni^{2+} and Al^{3+}. However, the extraction percentages of Ni and Al from spent catalyst after 120 min were 99.9% and 1%, respectively in 1 M HCl, under the leaching conditions: pulp density 0.2% (w/v), particle size 50-71 μm, temperature 323 K and stirring speed 500 rpm. The absence of the peaks corresponding to Ni in the leach residue obtained under these conditions also indicates the complete dissolution of Ni from the original spent catalyst. The leaching results obtained under different conditions by varying the acid concentration, temperature and particle size, follow a shrinking core kinetic model: $1 - (2/3)X - (1 - X)^{2/3} = k_{ap}t$. The increase in k_{ap} with increasing temperature corresponds to activation energy of 17 kJ/mol based on the Arrhenius plot and supports a diffusion controlled mechanism. Further evidence for a diffusion controlled reaction and

a shrinking core model is demonstrated by a linear dependence of k_{ap} on $1/d^2$ and a first order dependence of k_{ap} on HCl concentrations lower than 0.1 M.

Acknowledgements

The authors wish to thank Korea Institute of Geoscience and Mineral Resources (KIGAM), Daejeon, for the award of Post Doctoral Fellowship for P.K. Parhi. Financial assistance and support from the Parker CRC for Integrated Hydrometallurgy Solutions and Murdoch University are gratefully acknowledged.

References:

1. C.L. Thomas, Catalytic Process and Proven catalysts. Academic Press, New York and London 1970.
2. G.W. Bridger and G.C. Chinchen, Hydrocarbon Reforming Catalysts, in Catalyst Handbook, Wolfe Scientific Books, London (1970) 64-96.
3. S. Goel, K.K. Pant, K.D.P. Nigam, J. Hazard. Mater. 171 (2009) 253–261.
4. H.I. Kim, Kyung-Ho Park, Devabrata Mishra, Hydrometallurgy 98 (2009) 192–195.
5. M. Marafi, A. Stanislaus, Resour. Conserv. Recy. 52 (2008) 859–873.
6. J. Y. Lee, S. V. Rao, B. N. Kumar, D. J. Kang, B. R. Reddy, J. Hazard. Mater. 176 (2010) 1122–1125.
7. D. Rapaport, Hydrocarb. Process. 79 (2000) 49-53.
8. A. Szymczycha-Madeja, J. Hazard. Mater. 186 (2011) 2157-2161.
9. V. Bosio, M. Viera, E. Donati, J. Hazard. Mater. 154 (2008) 804–810.
10. R. G. Busnardo, N. G. Busnardo, G. N. Salvato, J. C. Afonso, J. Hazard. Mater., B139 (2007) 391–398.
11. J. Idris , M. Musa , C.Y. Yin , K. H. K. Hamid, J. Ind. Eng. Chem. 16 (2010) 251–255.

12. A.J. Chaudhary, J.D. Donaldson, S.C. Boddington and S.M. Grimes, Hydrometallurgy 34 (1993) 137-150.

13. A. Ognyanova, T. Ozturk, I.De. Michelis, F. Ferella, G. Taglieri, A. Akcil, F., Veglio, Hydrometallurgy 100 (2009) 20–28.

14. W. Mulak, B. Miazga, A. Szymczycha, Int. J. Miner. Process. 77 (2005) 231– 235.

15. N.M. Al-Mansi, N.M. Abdel Monem, Waste Manage. 22 (2002) 85–90.

16. P. Alex, T.K. Mukherjee and M. Sundaresan, Hydrometallurgy 34 (1993) 239-253.

17. E. Furimsky, Catal. Today 30 (1996) 223-286.

18. A. Roine, Outokumpu HSC Chemistry Thermochemical Database, Ver 6.1 (2002), Finland: Outokumpu Research Oy.

19. E.A. Abdel-Aal, M.M. Rashad, Hydrometallurgy 74 (2004) 189–194.

20. D. Georgiou, V.G. Papangelakis, Hydrometallurgy 49 (1998) 23–46.

21. X. Hou, L. Xiao, C. Gao, Q. Zhang, L. Zeng, Hydrometallurgy 104 (2010) 76–80.

22. X. Hou, L. Xiao, C. Gao, Q. Zhang, L. Zeng, Hydrometallurgy 104 (2010) 76–80.

23. F. Habashi, Gordon and Breach, Newyork, 1 (1969) 153-163.

24. S. Anand, R.P.Das, T. Indian I. Metals. 41(1988) 335-341.

25. L.T. Romankiw, D. Bruyn, Unit Process in Hydrometallurgy, Delas TX, (1963) 62.

26. P.R. Raisoni, S.G. Dixit, Miner.Eng. 1(1988) 225-234.

27. G. Senanayake, A. Senaputra, M.J. Nicol, Hydrometallurgy 105 (2010) 60-68.

28. G. Senanayake, G.K. Das, Hydrometallurgy 72 (2004) 59-72.

29. G. Senanayake, J. Childs, B.D. Akerstrom, D. Pugaev, Hydrometallurgy 110 (2011) 13-32.

List of table titles

List of figure captions

Table.1. Summary of leaching conditions

Figure	Particle size range (μm)	Pulp density % (w/v)	Temperature (K)	HCl concentration (M)	Stirring rate min^{-1}
3	-147	0.2 , 0.4	323	1	500
4	-147	0.2	323	1	200, 300, 400, 500, 600
5	-147	0.2	323	0.025, 0.05, 0.1, 0.5, 1 , 2	500
6	-147	0.2	293, 313, 323, 333, 353	1	500
7	50-71, 71-120, 125-150, 150-180	0.2	323	1	500

Total reaction time 180 min in all cases

Table.2.Chemical analysis of original spent catalyst

Element	Si	Ni	Al	Fe	Zn	Co	Ca	Mg	Mn	C	S	K	Na
%	0.1	12.75	39.2	0.68	0.21	0.012	2.28	0.1	0.039	0.7	0.005	0.36	0.12

Table 3. Thermodynamic data and equilibrium constants for acid dissolution of Ni and Al_2O_3

Reaction	T (K)	ΔH^o (kJ/mol)	ΔG^o (kJ/mol)	log K
$Ni + 2H^+ = Ni^{2+} + H_2(g)$	293	-53.8	-45.8	8.17
	323	-55.0	-44.9	7.27
	353	-56.0	-43.9	6.50
$Al_2O_3 + 6H^+ = 2Al^{3+} + 3H_2O$	293	-258	-115	20.5
	323	-261	-100	16.2
	353	-263	-85.5	12.6

Data from HSC 6.1 [18]

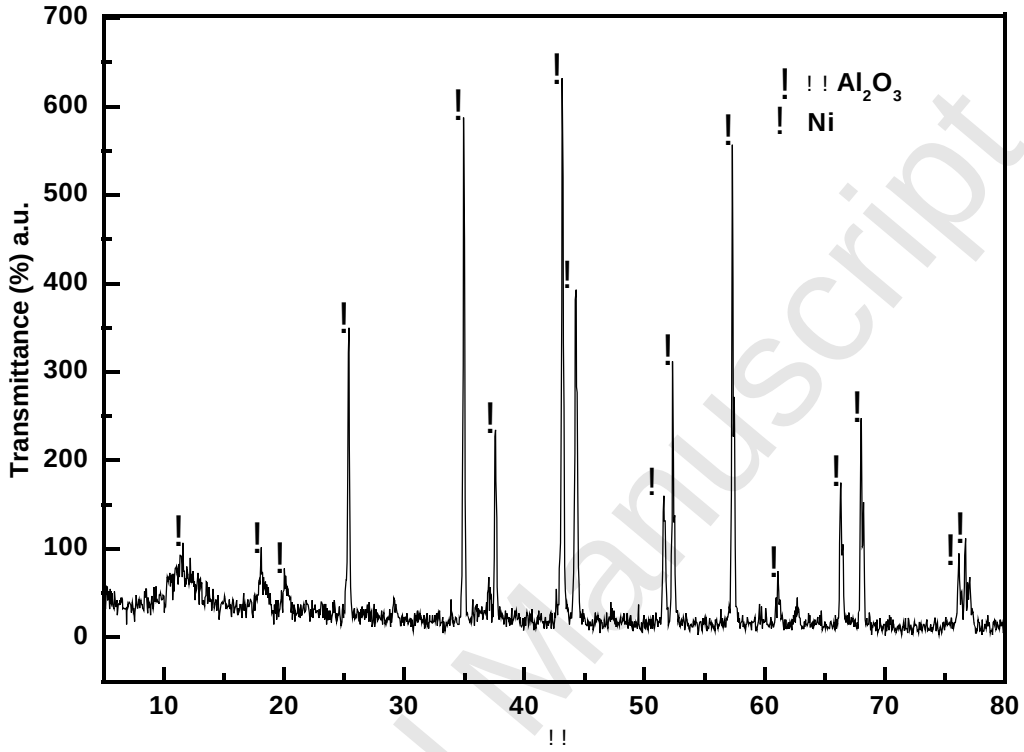

Fig.1. XRD analysis of original spent catalyst sample

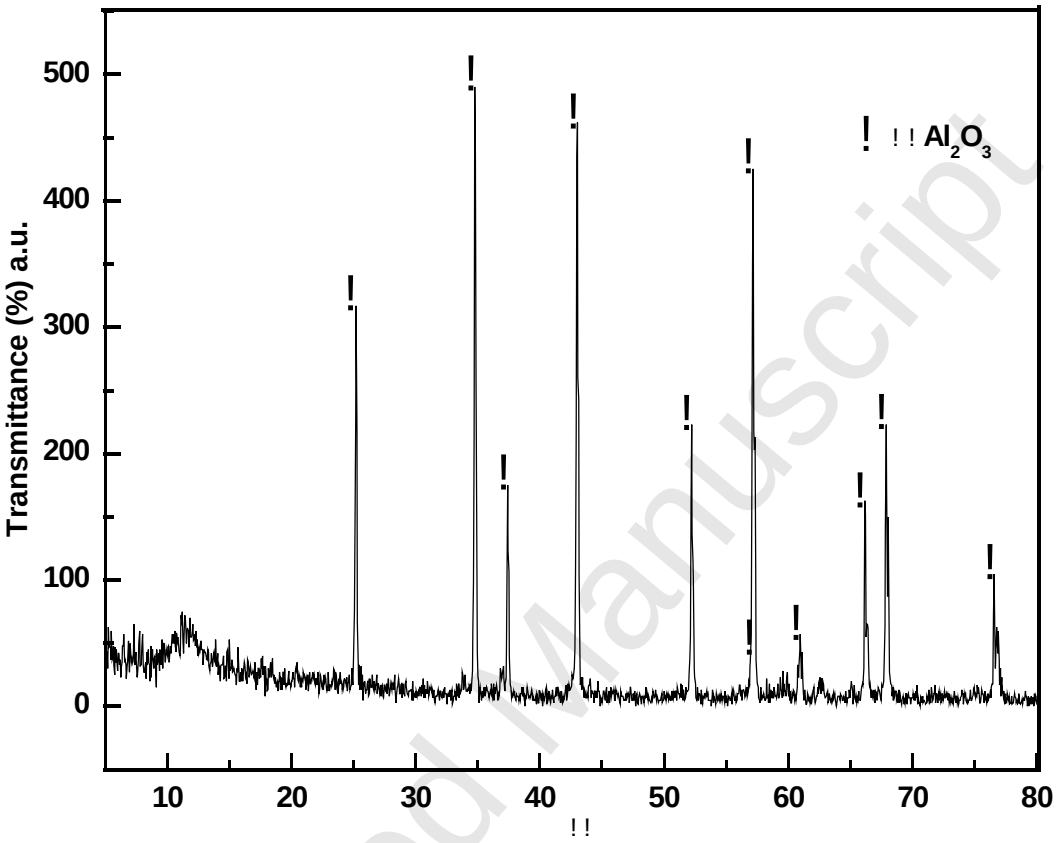

Fig.2. XRD analysis of a typical residue sample
(Condition: 0.2(w/v)%, 323 K, 50-71 μm, 1 M HCl, 500 rpm)

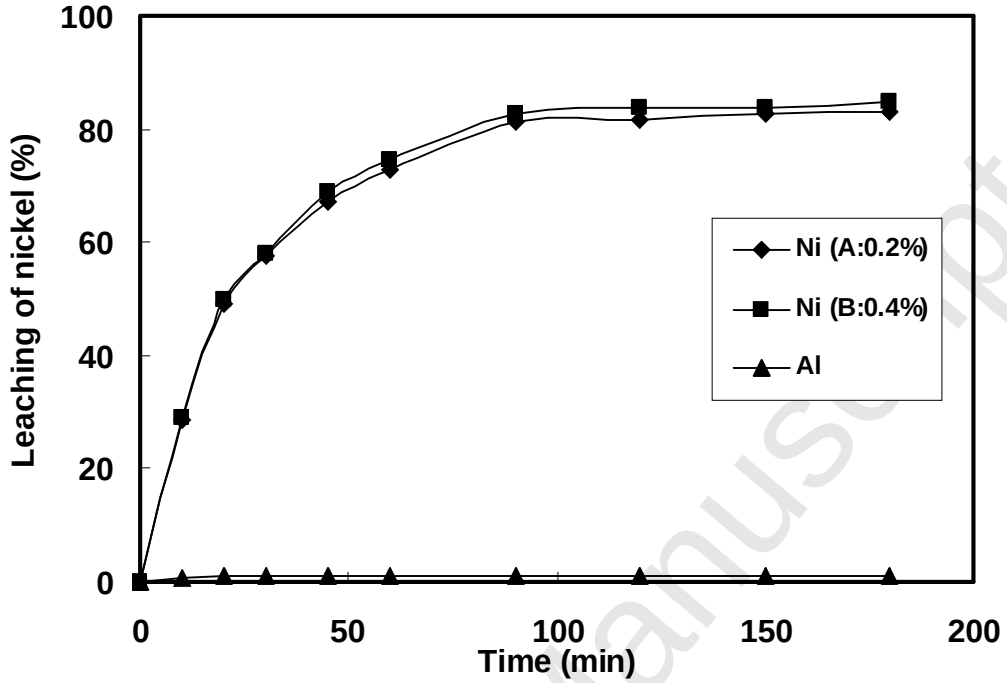

Fig.3. Effect of pulp density on nickel leaching (Conditions: 500 rpm, 323 K, 1 M HCl)

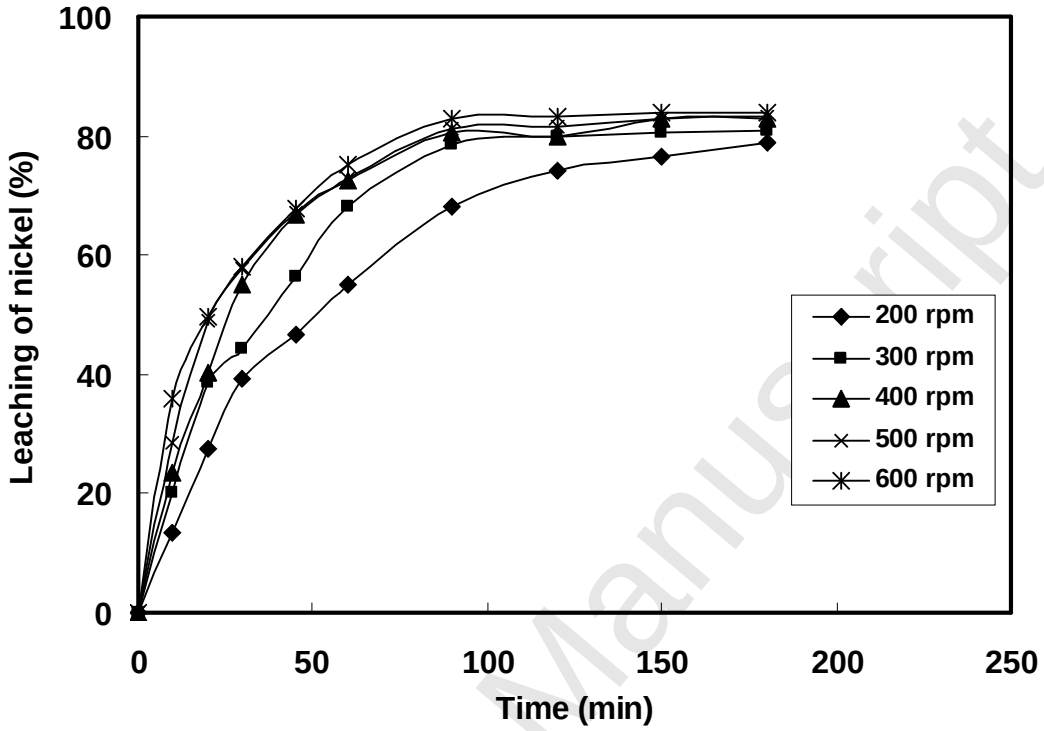

Fig.4. Effect of stirring speed on nickel leaching (Conditions: 0.2% (w/v), 323 K, 1 M HCl)

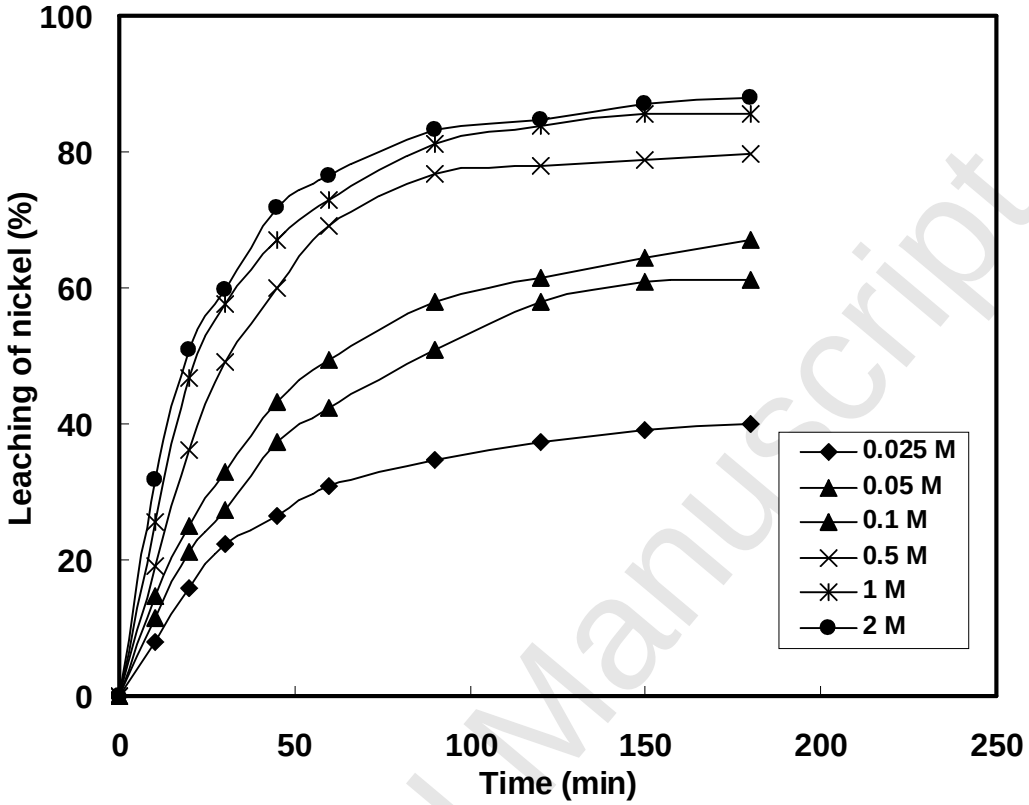

Fig.5. Effect of HCl concentration on nickel leaching
(Conditions: 0.2% (w/v), 323 K, 500 rpm)

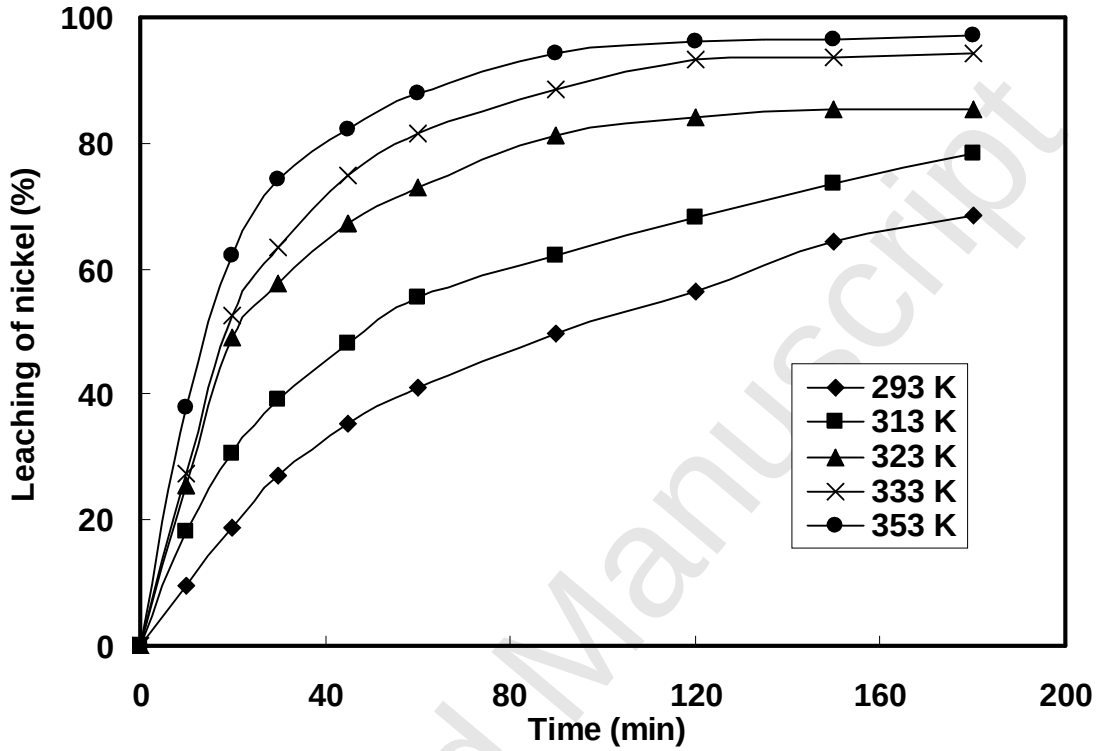

Fig.6. Effect of temperature on nickel leaching (Conditions: 0.2% (w/v), 1 M HCl, 500 rpm)

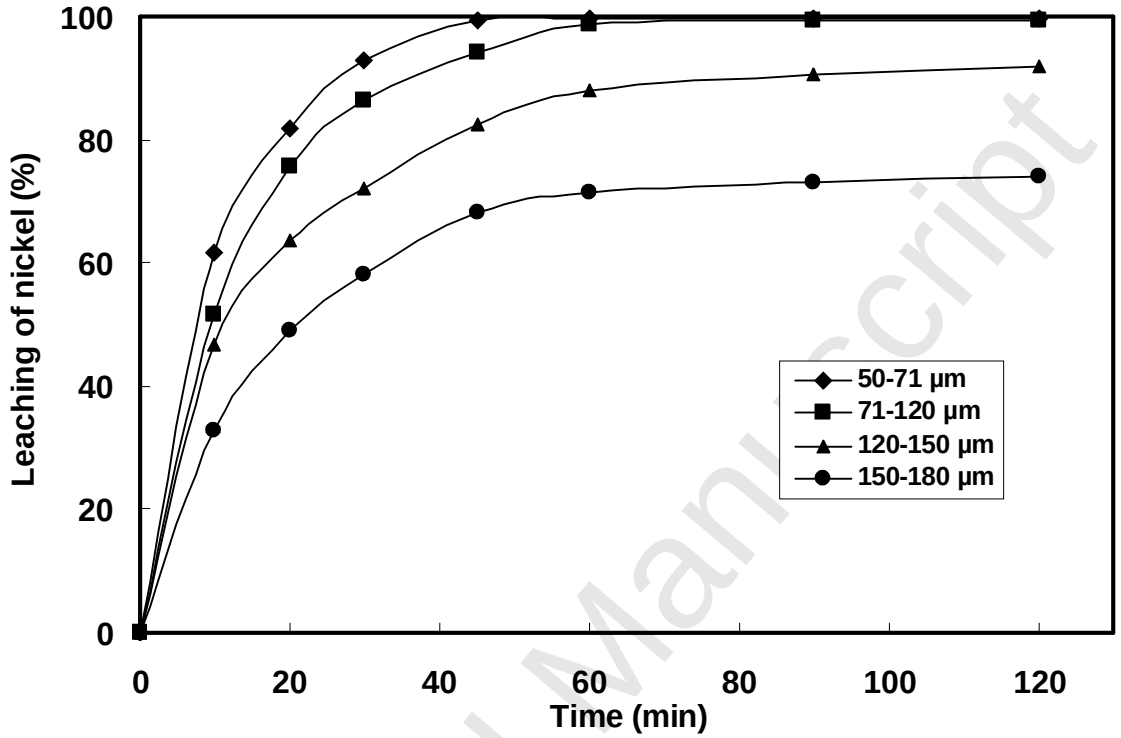

Fig.7. Effect of particle size on nickel leaching (Conditions: 0.2% (w/v), 323 K, 1 M HCl, 500 rpm)

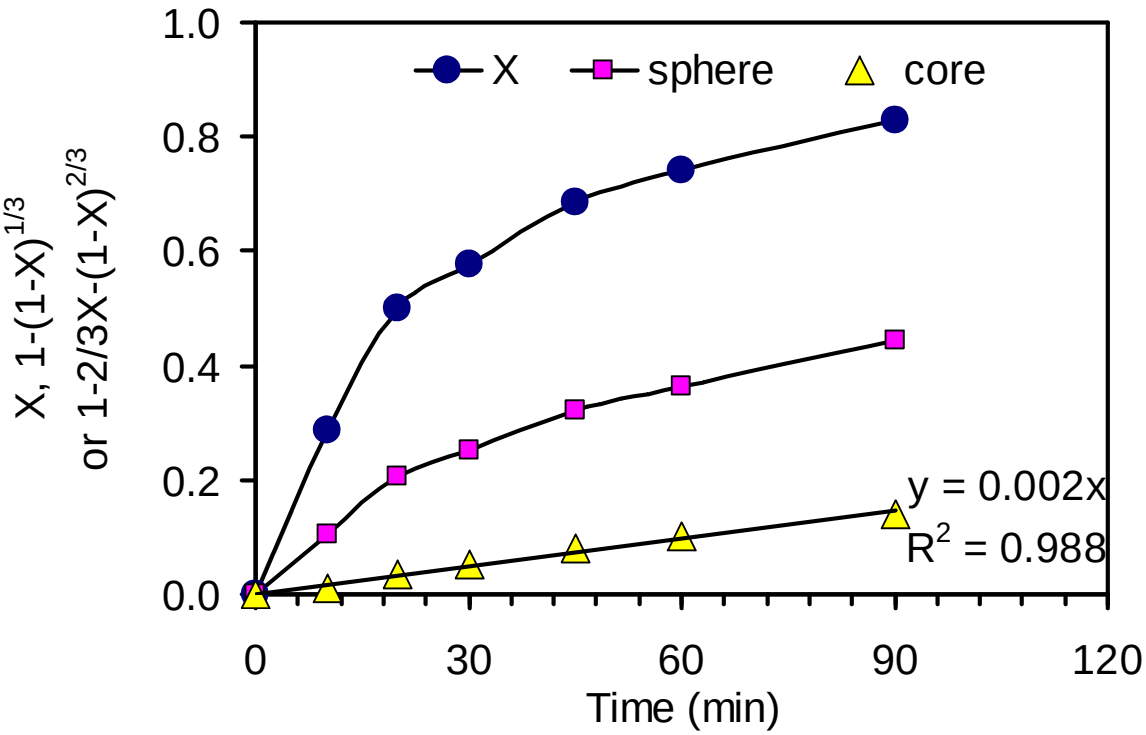

Fig.8. Applicability of a shrinking core kinetic model (Eq.3) to nickel leaching (Results from Fig. 3)

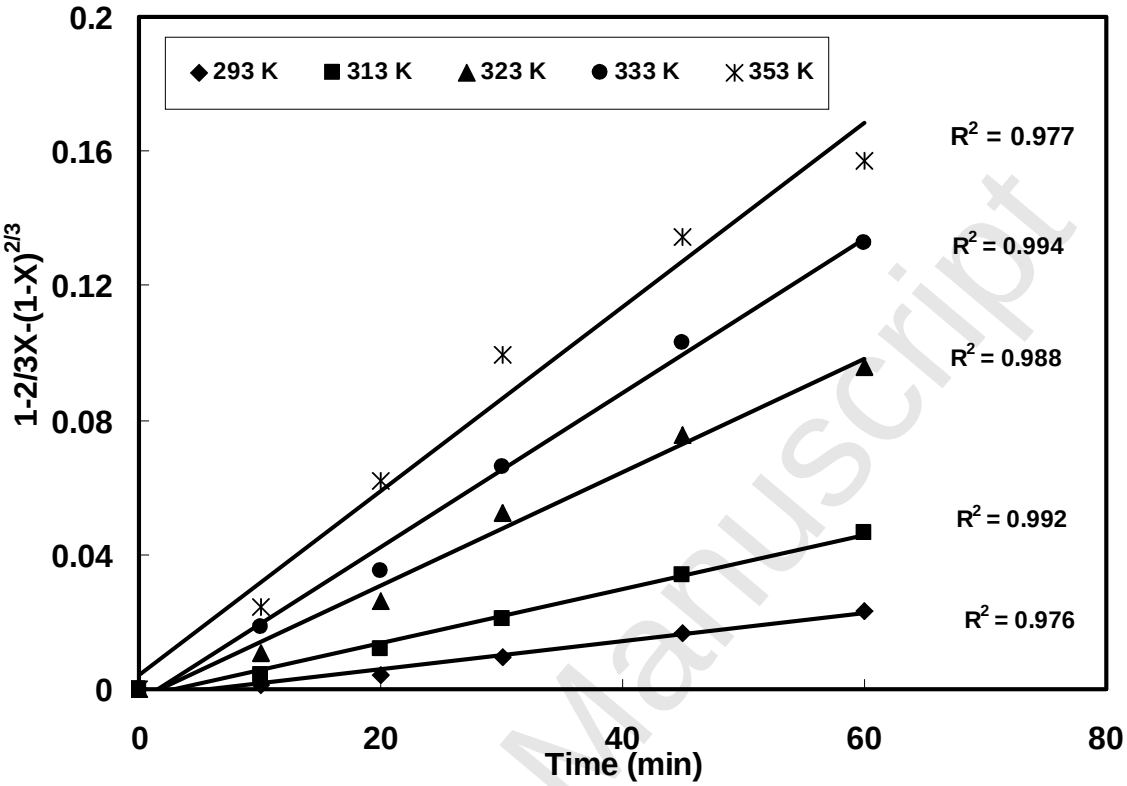

Fig.9. Applicability of a shrinking core kinetic model for nickel leaching at different temperatures (Results from Fig. 6)

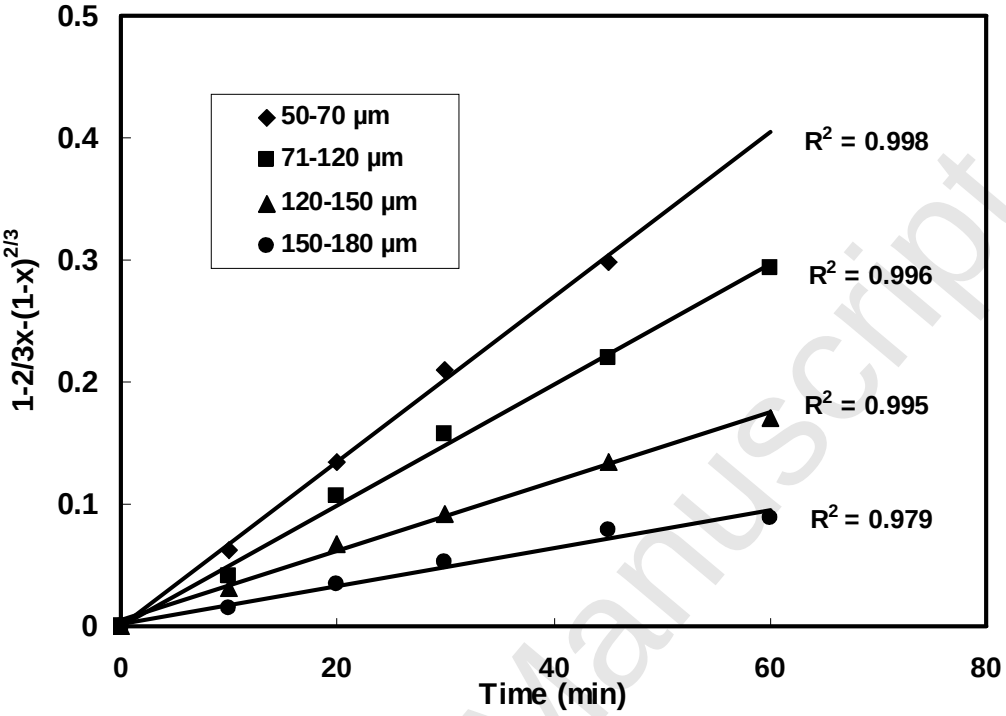

Fig.10. Applicability of a shrinking core kinetic model for nickel leaching from particles of different size (Results from Fig. 7)

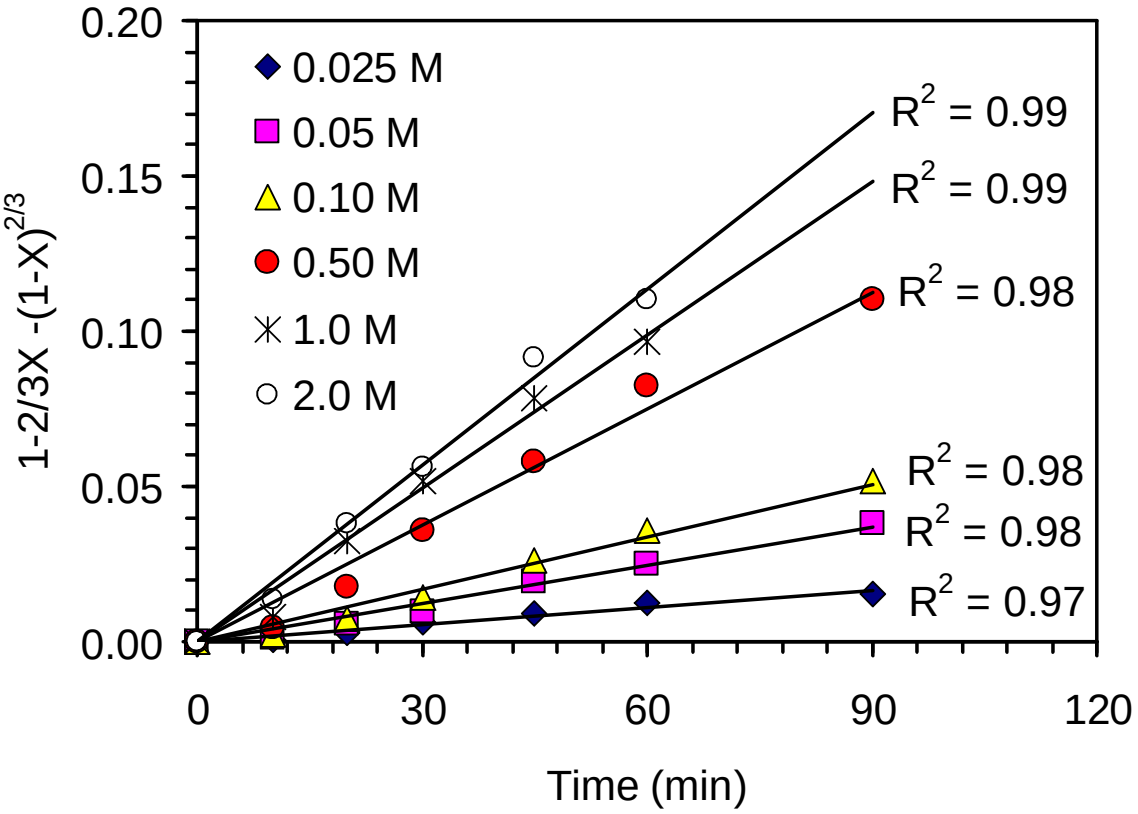

Fig.11. Applicability of a shrinking core kinetic model for nickel leaching at different HCl concentrations (Results from Fig. 8)

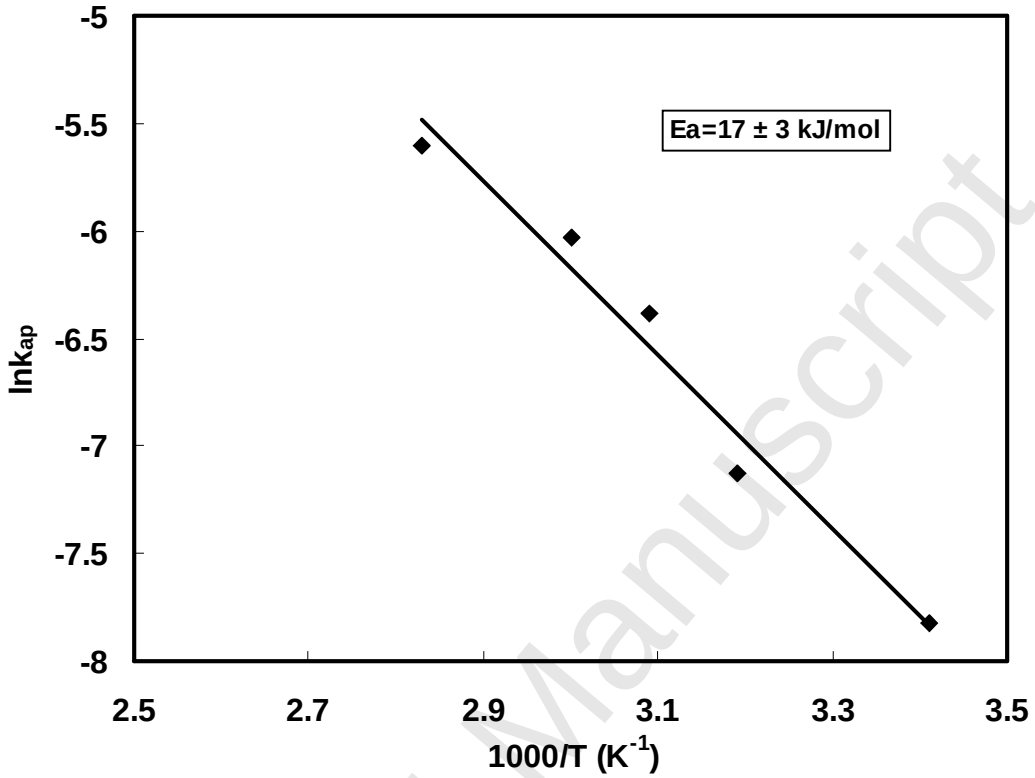

Fig.12. Arrhenius plot for nickel leaching (k_{ap} from Fig. 9)

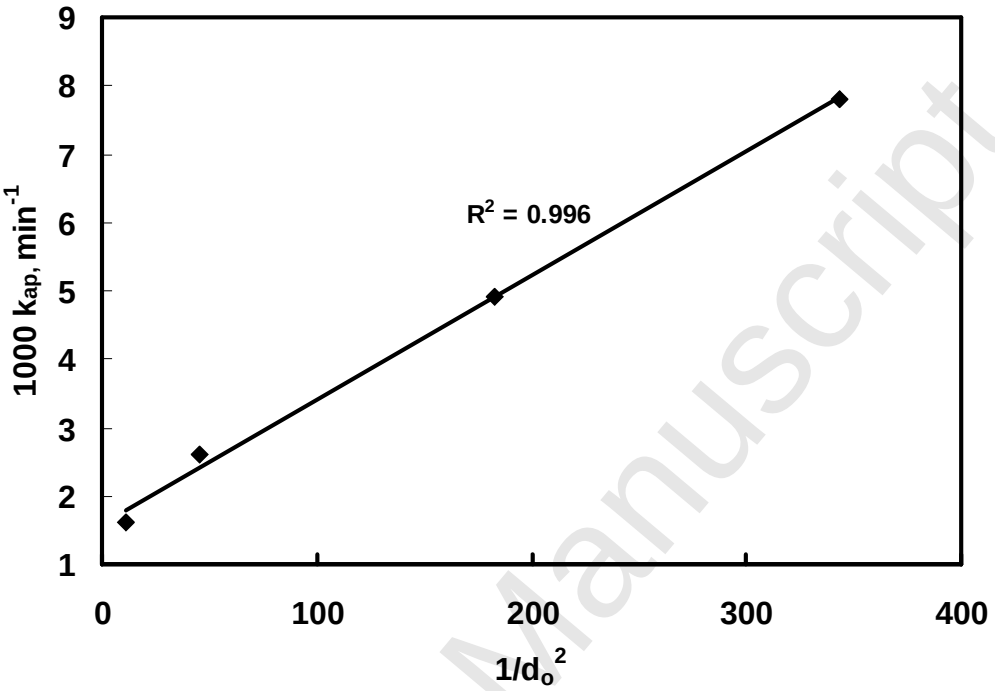

Fig.13. Plot of k_{ap} as a function of $1/d_o^2$ (k_{ap} from Fig. 10)

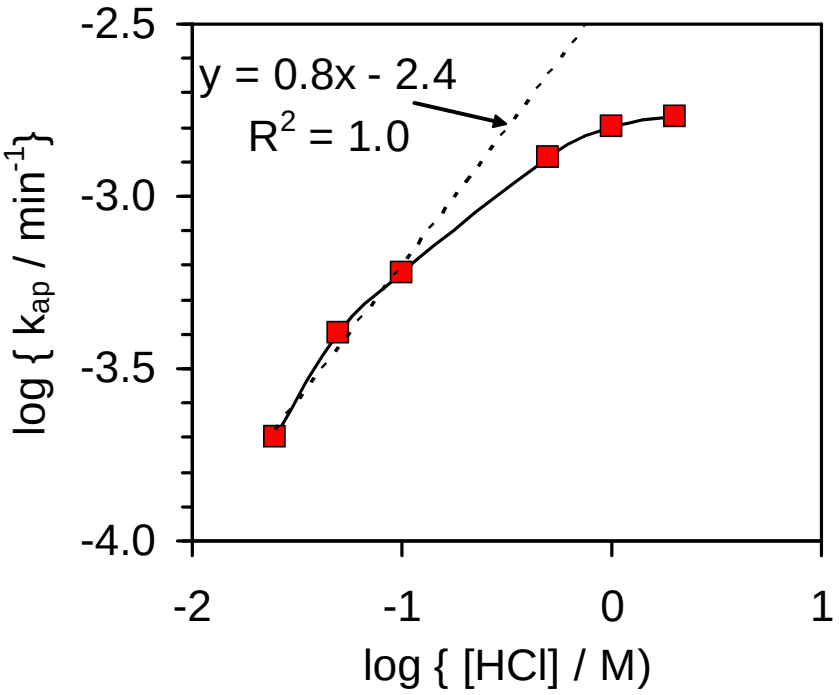

Fig.14. Plot of log k_{ap} as a function of log [HCl] (k_{ap} from Fig. 11)